Solid State Communications 303-304 (2019) 113740

Contents lists available at ScienceDirect

Solid State Communications

journal homepage: http://www.elsevier.com/locate/ssc

Communication

Structural, electronic, elastic and vibrational properties of two dimensional graphene-like BN under high pressure

Cihan Kürkçü [a,*], Çağatay Yamçıçıer [b]

[a] Department of Electronics and Automation, Kırşehir Ahi Evran University, 40100, Kırşehir, Turkey
[b] Institute of Science, Gazi University, 06500, Ankara, Turkey

ARTICLE INFO

Communicated by Ralph Gebauer

Keywords:
2d materials
Phase transition
Intermediate state
Electronic structure
Elastic constants
Phonon

ABSTRACT

The structural, electronic, elastic and vibrational properties of boron nitride (BN) were analyzed using ab initio computational methods based on density functional theory. The exchange-correlation energy functional was evaluated using the local density approximation (LDA) under pressure. BN crystallizes in hexagonal structure (h-BN) with symmetry $P6_3/mmc$. The structural transform was obtained at the BN from h-BN transformed into wurtzite (w-BN) with symmetry $P6_3mc$ at 12.5 GPa. During this phase transformation, intermediate states with space group $P\bar{3}m1$ and P3m1were observed. Besides, the electronic properties for the obtained stable phases of BN were calculated. Both structures have a semiconductor character with a direct band gap. We also made elastic and phonon calculations to understand the mechanical and dynamically stability of the obtained phases of BN. BN is stable in both phases. As a result of the literature searches, the obtained intermediate states were first predicted in this study. Thus, we believe that this study will guide the experimental studies to be conducted.

1. Introduction

In recent years, some theoretical [1–6] and experimental [7–16] studies have been carried out to investigate the physical and chemical properties of crystalline BN. BN is a III−V semiconductor compound with a structure very similar to graphite is a synthetically produced compound and has remarkable and useful properties in a wide range of applications such as deep ultraviolet emitter, transparent membrane, the dielectric layer, or protective coatings [17–19]. In previous studies on BN, it was revealed that the stable structure of BN was hexagonal in ambient conditions and the cubic and wurtzite structure was synthesized from the hexagonal structure at high temperature and pressure [7,8]. Some subsequent experimental studies have found that the cubic phase of BN is thermodynamically stable under ambient conditions and that hexagonal BN is stable at elevated temperatures ($T = 900–1500^{\circ}$) [12–14]. The possible scenarios on the transition of the phase stability from the hexagonal to the cubic structure are discussed, but this issue is inconclusive.

BN has four polymorphs: (I) the hexagonal structure (h-BN), analogous to graphite, with space group $P6_3/mmc$, (II) the rhombohedral structure (r-BN) with space group R3m. These structures have a two-dimensional (2D) layered structure consisting of sp^2 bonds. (III) the zinc blende structure (z-BN) with space group $F\bar{4}3m$, (IV) the wurtzite structure (w-BN) with space group $P6_3mc$. These structures have three-dimensional modifications consisting of sp^3 bonds and can be easily synthesized under high pressure and temperature [9,10,20–24].

In this study, we examined a graphite-like hexagonal structure which is the most stable phase of BN under high pressure. This structure of BN has a $P6_3/mmc$ space group in ambient conditions. It was observed that when the increased pressure was applied above this structure, the h-BN structure changed into another hexagonal wurtzite structure, the dense diamond-like modifications, with space group $P6_3mc$ [2,9,10]. Two trigonal intermediate states with space groups $P\bar{3}m1$ and P3m1 were predicted during this transition.

We calculated the electronic properties for both phases of BN. The h-BN and w-BN forms of BN have a wide band gap. They can be used in many technological fields with this feature. We have also calculated elastic and vibrational properties to determine the mechanical and dynamically stability of obtained phases of BN.

Besides, the graphene layers have three different stacking modes. AA-stacking with a simple hexagonal structure, AB-stacking with orthorhombic structure and ABC-stacking with rhombohedral structure. There is a small energy barrier between the AB- and AA-stacking. Therefore, in general, natural graphite adopts the AB-stacking

* Corresponding author.
E-mail address: ckurkcu@ahievran.edu.tr (C. Kürkçü).

https://doi.org/10.1016/j.ssc.2019.113740
Received 11 July 2019; Received in revised form 28 August 2019; Accepted 25 September 2019
Available online 26 September 2019

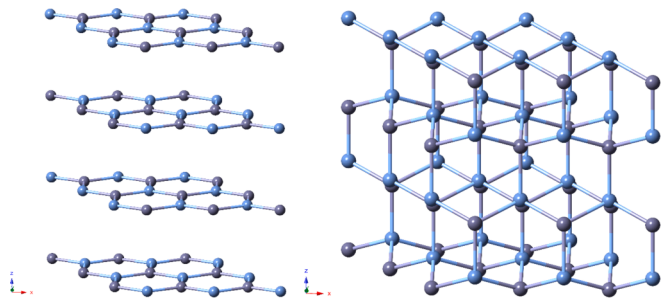

Fig. 1. The graph of the change of simulation cell volume as the function of the pressure.

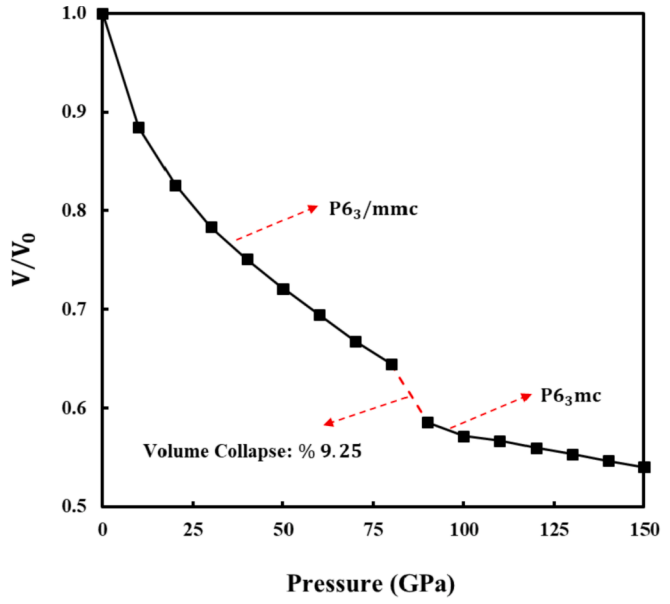

Fig. 2. Crystal structures of BN: $P6_3/mmc$ phase of BN (left) at zero pressure and $P6_3mc$ phase of BN (right) at 90 GPa.

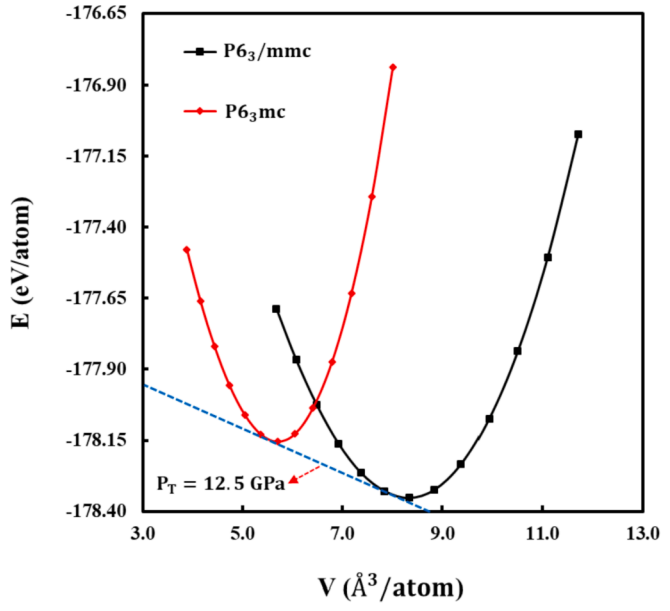

Fig. 3. Energy-volume graph for the stable phases of the BN compound.

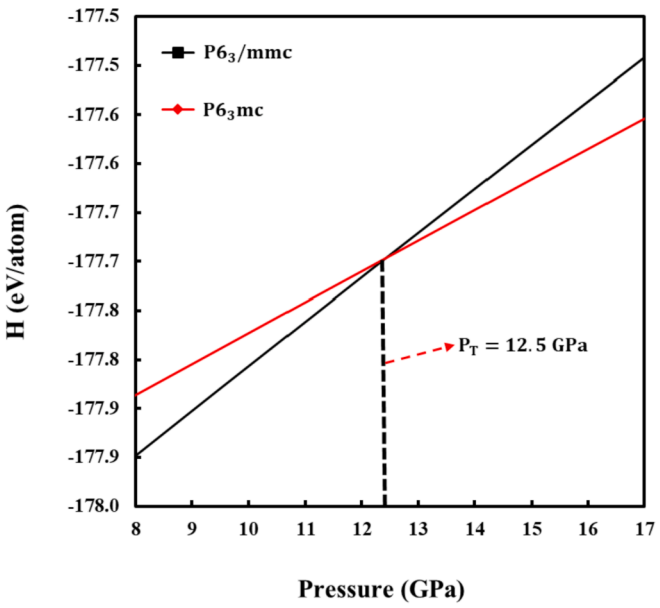

Fig. 4. Enthalpy graph for the stable phases of BN as the function of the pressure.

sequence [25] and there are also many theoretical and experimental studies on the AB-stacking sequence [26–33]. On the other hand, due to the lack of practical samples and associated with experimental observations, there is little theoretical work on the AA-stacking [34,35]. Very recently, however, Liu et al. [36] surprisingly found that bilayer graphene shows AA-stacking, which is often difficult to distinguish from monolayer graphene. As a result, it is necessary to do more research, both theoretically and experimentally, on the physical properties of AA-stacking BN [37].

Therefore, in this paper, we will perform ab-initio calculations on structural, electronic, mechanic and vibrational properties of AA stacking BN. We believe that our results will guide people who want to work experimentally.

2. Methods

The structural, electronic, elastic and vibrational properties of BN were carried out within Density Functional Theory (DFT) calculations using Siesta software package [38]. The calculations were performed using an LDA-CA exchange-correlation functional [39]. We have used Troullier-Martins type norm-conserving pseudo-potential for B and N atoms [40]. In all calculations were conducted using double-zeta plus polarized (DZP) basis sets of localized atomic orbitals. The energy mesh cut-off, which corresponds to the spacing of the real space grid used to calculate the Hartree, exchange, and correlation contribution to the total energy and Hamiltonian, was set to be 350 Rydberg (Ry). BN was modelled using 3x3x2 cells with periodic boundary condition for 72 atoms supercells. The Brillouin zones (BZ) were sampled with the 10x10x4 Monkhorst-Pack k-point mesh [41]. Structural optimizations were performed via the conjugate-gradient (CG) method until the residual force acting on all atoms were smaller than 0.01 eV/Å and pressure is gradually increased by 10 GPa through this method to the system. For analyze each minimization step, we used the KPLOT program and the RGS algorithm that give detailed information about the space groups, atomic positions and lattice parameters of an analyzed structure [42,43].

3. Results and discussions

BN with lattice parameters a = b = 2.4880 Å and c = 6.2543 Å under

Table 1
The values of transition pressure, lattice parameter, c/a ratio, volume, bulk modulus and derivate of bulk modulus for $P6_3/mmc$ and $P6_3mc$ phases of BN.

Phases	P_T (GPa)	a = b (Å)	c (Å)	c/a	V (Å^3/atom)	B_0 (GPa)	$B_0^{'}$	References
$P6_3/mmc$	0	2.4880	6.2543	2.5138	8.380	202.87	3.8272	This study
		2.4890	6.5010	2.6118	8.630	145.00		[52]
		2.5130	6.4330	2.5600	8.802	185.30		[53]
		2.4940	6.6600	2.6704		335.00	2.4800	[54]
$P6_3mc$	12.5	2.5244	4.1619	1.6487	5.740	410.16	3.4301	This study
		2.4700	3.9800	1.6070		406.00	3.8600	[55]
	14.0	2.5500	4.2000					[56]
		2.5360	4.1900			390.00	6.3000	[54]
		2.5580	4.2280	1.6530		376.31	3.5820	[57]
	8.5							[58]
	10.4							[59]

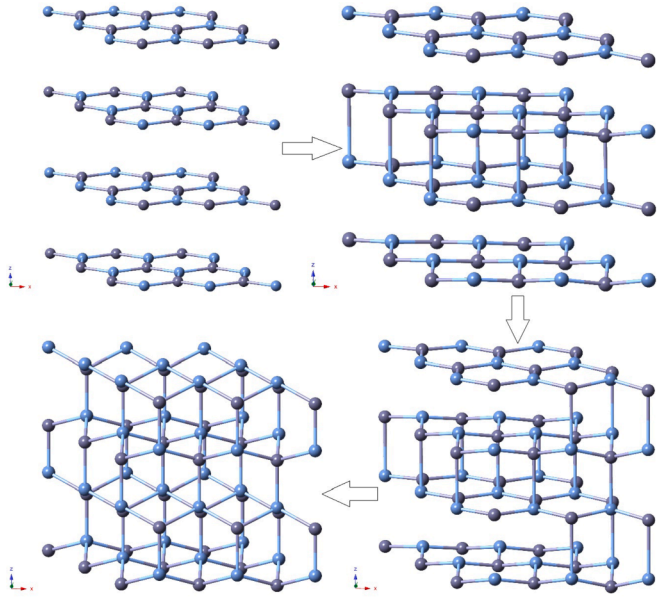

Fig. 5. Formation of $P6_3mc$ phase of BN at 90 GPa.

a pressure of 0 GPa crystallizes in hexagonal type structure with space group $P6_3/mmc$ and has 4 atoms in the unit cell. The B atoms are occupied the Wyckoff 2d (1/3, 2/3, 3/4) positions while the N atoms are occupied the Wyckoff 2c (1/3, 2/3, 1/4) positions. In this study, the BN compound was first equilibrated after optimizing and then gradually increased pressures of 10 GPa up to a pressure value of 150 GPa (0, 10, 20, 30 … 150 GPa) were applied to the equilibrium structure. We observed that when increasing pressure was applied on the structure of BN having the $P6_3/mmc$ space group, it turned into another hexagonal wurtzite type structure having a = b = 2.5244 Å and c = 4.1619 Å lattice parameters at 90 GPa. This structure has $P6_3mc$ space group. These structures obtained under high pressure are given in Fig. 1.

In order to examine the thermodynamic nature of the phase transformation obtained in the presence of a pressure of 90 GPa, reduced volume values corresponding to each pressure applied to the system were obtained. Using the obtained data, the pressure-reduced volume graph was plotted and given in Fig. 2. As can be seen from Fig. 2, there is a significant decrease in volume during the phase transition. This sharp decrease indicates that the phase transformation is first degree.

To determine which of the structures obtained for the BN compound is most stable, we discussed the changes in energy and volume at this stage of the study, and as a result of the calculations, we plotted the energy-volume curve given in Fig. 3. The data obtained in the calculations were fit to the third-order Birch-Murnaghan equation of state [44, 45] given in below.

$$P = 1.5B_0\left[\left(\frac{V}{V_0}\right)^{-\frac{7}{3}} - \left(\frac{V}{V_0}\right)^{-\frac{5}{3}}\right] x\left\{1 + 0.75\left(B_0^{'} - 4\right)\left[\left(\frac{V}{V_0}\right)^{-\frac{2}{3}} - 1\right]\right\} \quad (1)$$

where P is the pressure, V is the deformed volume, V_0 is the reference volume, B_0 is the bulk modulus, and $B_0^{'}$ is pressure derivative of the bulk modulus.

The transition pressure value obtained under the hydrostatic pressure is generally higher than the transition pressure value obtained from the experimental studies. As a result of the simulation, the system is faced with a significant energy barrier at the transition from one phase to another phase and tries to pass this barrier to achieve the phase transition. Thus, the system is exposed to excessively pressure [46–49].

The Gibbs free energy was used to determine the most thermodynamically stable phase at the given pressure and temperature. The Gibbs free energy is given as follows.

$$G = E_{tot} + PV - TS \quad (2)$$

E is the total energy, P is the pressure, V is the volume and S is the entropy. This study was carried out in the presence of 0 K temperature. Thus, in the Gibbs free energy given in Equation (2), the term TS disappears and it is equal to the enthalpy given by equation (3).

$$H = E_{tot} + PV \quad (3)$$

where $P = dE_{tot}/dV$.

Instead of the high-pressure value obtained by simulation, we can now obtain the transition pressure values which are in good agreement with the experimental results. The intersection of the enthalpy curve obtained for both $P6_3/mmc$ and $P6_3mc$ phases gives us the phase transition pressure value. To determine this value which is consistent with the experimental results, we plotted the pressure versus enthalpy graph in Fig. 4 and observed the transition pressure value as 12.5 GPa. In Table 1, the values of transition pressure, lattice parameters, c/a ratio, volume, bulk modulus and derivate of bulk modulus for h-BN and w-BN are given and compared with other studies in the literature.

Each minimization step of the w-BN structure was analyzed in detail using the KPLOT program to determine whether there was an intermediate state during this phase change obtained at 90 GPa. As a result of the analysis, we suggest that the w-BN structure proceeds through intermediate states with space groups $P\bar{3}m1$ (the calculated lattice parameters are $a = 2.4050$ Å, $b = 2.4050$ Å, $c = 4.2116$ Å, $\alpha = \beta = 90$ and $\gamma = 120^{\circ}$, in which two atoms B and N occupy the Wyckoff 2d (1/3, 2/3, z), z = 0.727156 and 2d (1/3, 2/3, z), z = 0.246728 sites, respectively.) at 32nd step and with space groups P3m1 (the calculated lattice parameters are $a = 2.4028$ Å, $b = 2.4028$ Å, $c = 4.1494$ Å, $\alpha = \beta = 90$ and $\gamma = 120^{\circ}$, in which B atoms occupy the Wyckoff 1a (0, 0, z), z = 0 and 1c (2/3, 1/3, z), z = 0.558689 sites and N atoms occupy the Wyckoff 1a (0, 0, z), z = 0.569511 and 1c (2/3, 1/3, z), z = 0.069978 sites) at 38th step. Thus, the transition path for BN was obtained as $P6_3/mmc \rightarrow P\bar{3}m1 \rightarrow$

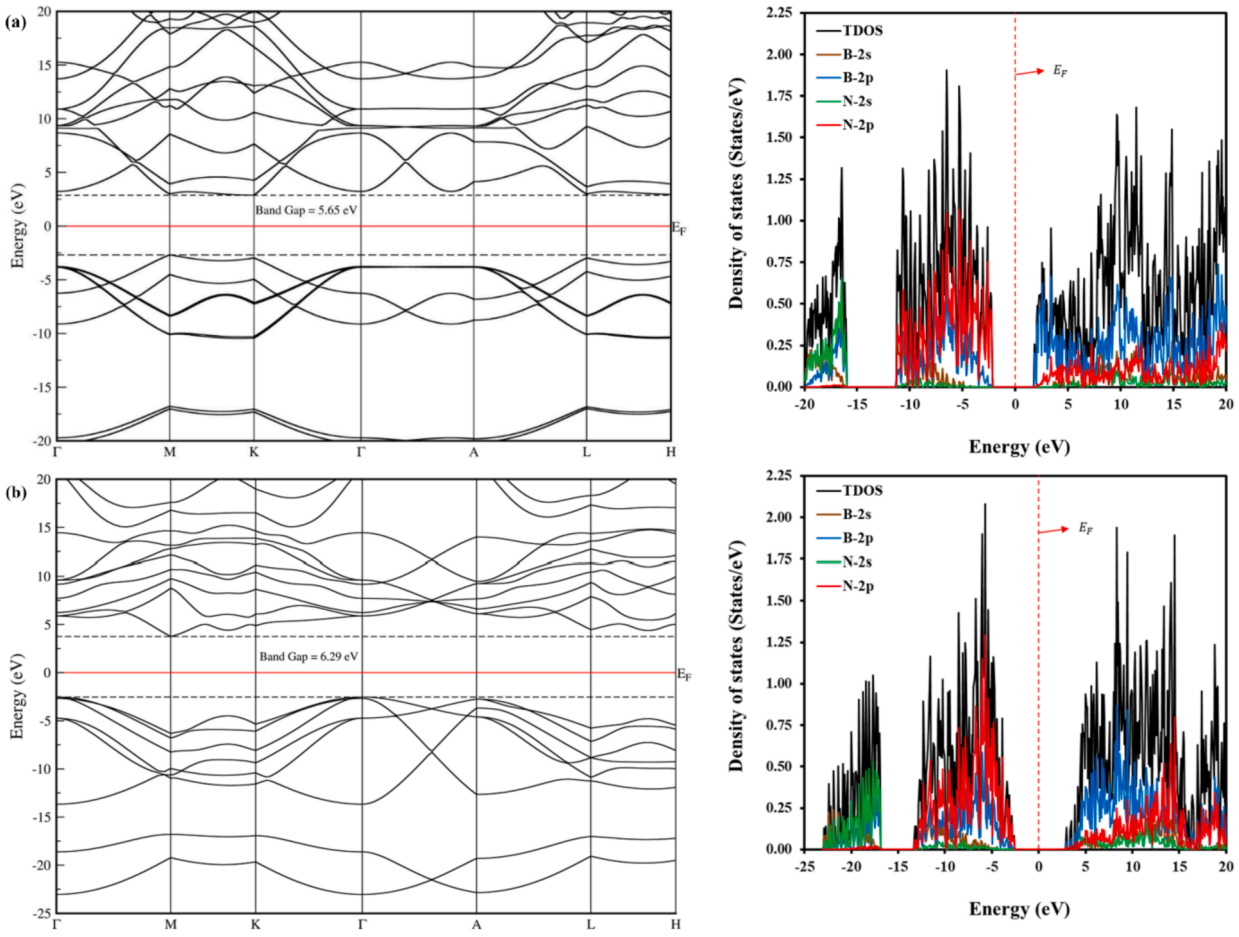

Fig. 6. Band structure and density of states curves for BN a) $P6_3/mmc$ and b) $P6_3mc$ phase.

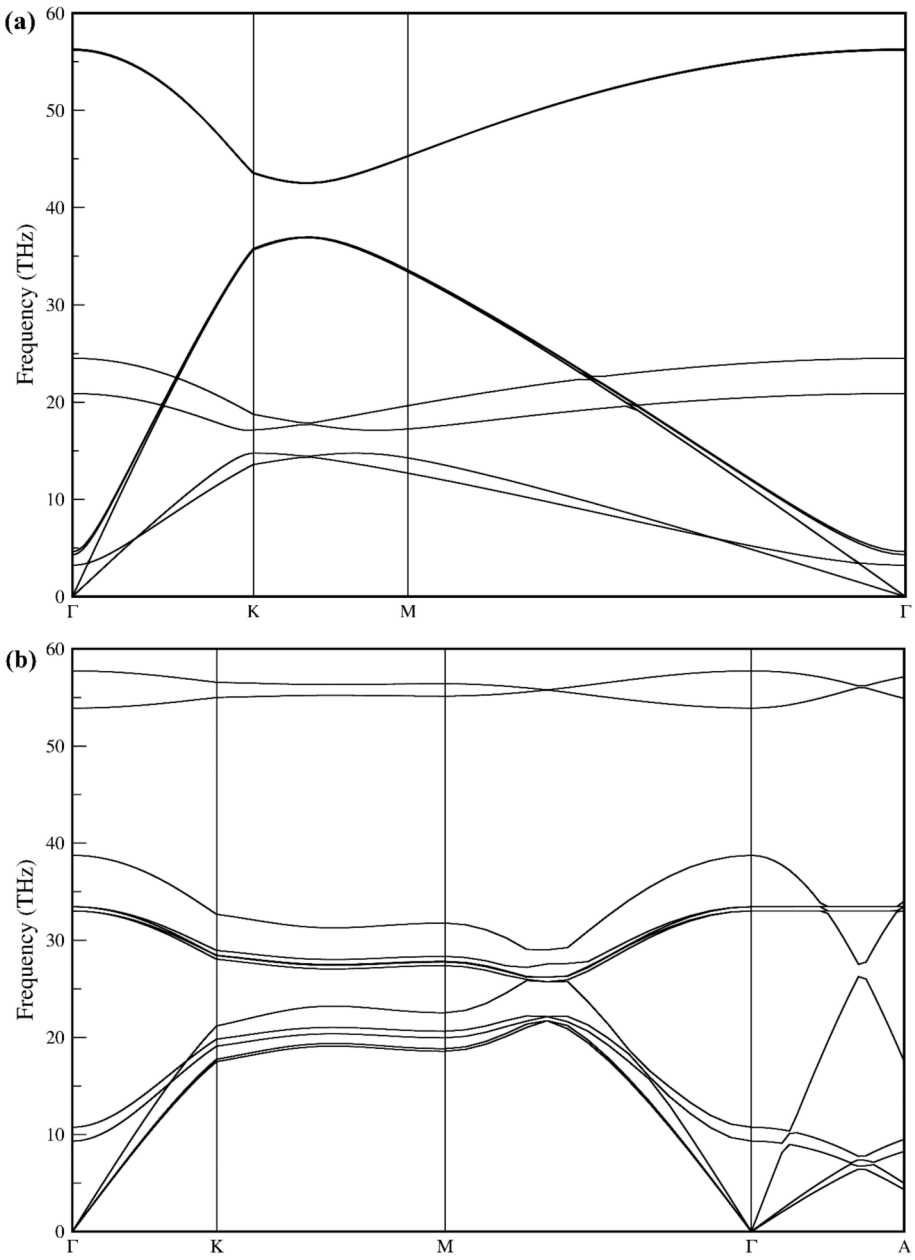

Fig. 7. The phonon dispersion curves for BN a) $P6_3/mmc$ and b) $P6_3mc$ phase.

Table 2
Elastic constants (C_{ij} in GPa) for $P6_3/mmc$ and $P6_3mc$ phases of BN.

Phases	C_{11}	C_{12}	C_{13}	C_{33}	C_{44}	References
$P6_3/mmc$	742.53	164.29	2.4281	2.5197	6.1322	This study
	901.00	202.00	2.2000	26.600	5.2000	[60]
	927.00	223.00	1.0000	32.0000	7.0000	[52]
$P6_3mc$	1001.2	152.8	70.727	1100.4	424.22	This study
	944.0	149.0	83.000	1011.0	350.00	[61]
	954.9	143.0	79.100	1018.9	357.30	[62]
	990.0	148.0	63.000	1090.0	345.00	[63]

P3m1 →$P6_3mc$ and depicted in Fig. 5 for the evolution of the w-BN structure.

We calculated the electronic band structures along with the high-symmetry directions and corresponding total and partial DOS as a function of energy for $P6_3/mmc$ and $P6_3mc$ phases of BN. These were illustrated near the Fermi energy (E_F) level in Fig. 6 a and b for $P6_3/mmc$ phase and $P6_3mc$ phases, respectively. Fermi levels were set to be 0 eV. The symmetry points were Γ – M – K – Γ – A – L – H for both h-BN and w-BN structure. According to Fig. 6, BN is a typical semiconductor, which exhibit an indirect band gap with an energy of 5.65 eV at $M \rightarrow K$ points for $P6_3/mmc$ phase and 6.29 eV at $\Gamma \rightarrow M$ points for $P6_3mc$ phase [50].

Furthermore, as can be seen in Figs. 6 and 7, for both $P6_3/mmc$ and $P6_3mc$ phase, the largest contribution in the range of $0 - (-10)$ below the Fermi energy level came from the N-2p state. In the case of lower energy values, it came from N-2s. Above Fermi energy level, the largest contribution came from B-2p.

Elastic constants (C_{ij}) are the important properties of solids, which determine the mechanical stability of crystals. So, we also calculated the elastic constants to investigate the mechanical stability of the obtained phases of BN. The obtained C_{ij} values are given in Table 2 and compared with other studies. The well-known conditions for the mechanical stability of hexagonal structures are: $C44 > 0$, $C_{11} > |C_{12}|$, $(C_{11}+2C_{12})C_{33} > 2C_{13}^2$ [51]. Our results given in Table II, satisfy these stability conditions for the h-BN and w-BN structures. So, these structures are

mechanically stable.

The calculated phonon-dispersion curves are shown in Fig. 7 a and b for $P6_3/mmc$ and $P6_3mc$ phases of BN, respectively. Since unit cells of $P6_3/mmc$ and $P6_3mc$ phases contain four atoms, the corresponding number of vibration modes is twelve, as seen in Fig. 7, of which three are acoustic branches and the remaining nine are optical modes. We do not find any imaginary phonon frequency in the whole Brillouin zone for $P6_3/mmc$ and $P6_3mc$ phases. This supports that $P6_3/mmc$ and $P6_3mc$ phases of BN are the dynamical stability.

4. Conclusions

In this study, ab-initio calculations were performed to examine phase transition behaviour of BN under high pressure with SIESTA. As a result of the calculations, a first-order phase transition was observed from the $P6_3/mmc$ phase to the $P6_3mc$ phase. Besides, two different intermediate states were predicted during this phase transition. These intermediate states were firstly predicted in this study. On the other hand, to much understand the physical properties of BN, electronic band structure and density of states were examined. Both $P6_3/mmc$ and $P6_3mc$ phases of BN have a semiconductor character. We also calculated elastic constants and vibrational properties of BN and found both phases mechanically and dynamically stable.

References

[1] K. Albe, Theoretical study of boron nitride modifications at hydrostatic pressures, Phys. Rev. B 55 (10) (1997) 6203.
[2] M. Durandurdu, Amorphous boron nitride at high pressure, Philos. Mag. 96 (18) (2016) 1950–1964.
[3] J. Furthmüller, J. Hafner, G. Kresse, Ab initio calculation of the structural and electronic properties of carbon and boron nitride using ultrasoft pseudopotentials, Phys. Rev. B 50 (21) (1994) 15606.
[4] A. Janotti, S.-H. Wei, D. Singh, First-principles study of the stability of BN and C, Phys. Rev. B 64 (17) (2001) 174107.
[5] G. Kern, G. Kresse, J. Hafner, Ab initio calculation of the lattice dynamics and phase diagram of boron nitride, Phys. Rev. B 59 (13) (1999) 8551.
[6] W. Yu, et al., Ab initio study of phase transformations in boron nitride, Phys. Rev. B 67 (1) (2003), 014108.
[7] F. Bundy, J. Kasper, Hexagonal diamond—a new form of carbon, J. Chem. Phys. 46 (9) (1967) 3437–3446.
[8] F. Bundy, Pressure-temperature phase diagram of elemental carbon, Phys. A Stat. Mech. Appl. 156 (1) (1989) 169–178.
[9] F. Bundy, R. Wentorf Jr., Direct transformation of hexagonal boron nitride to denser forms, J. Chem. Phys. 38 (5) (1963) 1144–1149.
[10] F. Corrigan, F. Bundy, Direct transitions among the allotropic forms of boron nitride at high pressures and temperatures, J. Chem. Phys. 63 (9) (1975) 3812–3820.
[11] C. Yoo, et al., Direct elementary reactions of boron and nitrogen at high pressures and temperatures, Phys. Rev. B 56 (1) (1997) 140.
[12] S. Bohr, R. Haubner, B. Lux, Comparative aspects of c-BN and diamond CVD, Diam. Relat. Mater. 4 (5–6) (1995) 714–719.
[13] H. Sachdev, et al., Investigation of the c-BN/h-BN phase transformation at normal pressure, Diam. Relat. Mater. 6 (2–4) (1997) 286–292.
[14] V. Solozhenko, Current trends in the phase diagram of boron nitride, J. Hard Mater. 6 (1995) 51–65.
[15] V. Solozhenko, New concept of BN phase diagram: an applied aspect, Diam. Relat. Mater. 4 (1) (1994) 1–4.
[16] V.L. Solozhenko, V.Z. Turkevich, W.B. Holzapfel, Refined phase diagram of boron nitride, J. Phys. Chem. B 103 (15) (1999) 2903–2905.
[17] Y. Kubota, et al., Deep ultraviolet light-emitting hexagonal boron nitride synthesized at atmospheric pressure, Science 317 (5840) (2007) 932–934.
[18] T. Sugino, T. Tai, Dielectric constant of boron nitride films synthesized by plasma-assisted chemical vapor deposition, Jpn. J. Appl. Phys. 39 (11A) (2000) L1101.
[19] K. Watanabe, T. Taniguchi, H. Kanda, Direct-bandgap properties and evidence for ultraviolet lasing of hexagonal boron nitride single crystal, Nat. Mater. 3 (6) (2004) 404.
[20] V. Solozhenko, F. Elf, On the threshold pressure of the hBN-to-wBN phase transformation at room temperature, JOURNAL OF SUPERHARD MATERIALS C/C OF SVERKHTVERDYE MATERIALY 20 (1998) 62–63.
[21] V. Solozhenko, G. Will, F. Elf, Isothermal compression of hexagonal graphite-like boron nitride up to 12 GPa, Solid State Commun. 96 (1) (1995) 1–3.
[22] V.I. Levitas, et al., Strain-induced disorder, phase transformations, and transformation-induced plasticity in hexagonal boron nitride under compression and shear in a rotational diamond anvil cell: in situ x-ray diffraction study and modeling, J. Chem. Phys. 125 (4) (2006), 044507.
[23] Y. Meng, et al., The formation of sp 3 bonding in compressed BN, Nat. Mater. 3 (2) (2004) 111.
[24] V. Britun, et al., Formation of diamond-like BN phases under shock compression of graphite-like BN with different degree of structural ordering, Diam. Relat. Mater. 16 (2) (2007) 267–276.
[25] J.-C. Charlier, J.-P. Michenaud, X. Gonze, First-principles study of the electronic properties of simple hexagonal graphite, Phys. Rev. B 46 (8) (1992) 4531.
[26] C. Lu, et al., Low-energy electronic properties of the AB-stacked few-layer graphites, J. Phys. Condens. Matter 18 (26) (2006) 5849.
[27] C. Lu, et al., Influence of an electric field on the optical properties of few-layer graphene with AB stacking, Phys. Rev. B 73 (14) (2006) 144427.
[28] J.R. Huang, et al., Structural and electronic properties of few-layer graphenes from first-principles, Phys. Status Solidi 245 (1) (2008) 136–141.
[29] L. Falkovsky, Optical properties of doped graphene layers, J. Exp. Theor. Phys. 106 (3) (2008) 575–580.
[30] K.F. Mak, et al., Measurement of the optical conductivity of graphene, Phys. Rev. Lett. 101 (19) (2008) 196405.
[31] Z. Li, et al., Dirac charge dynamics in graphene by infrared spectroscopy, Nat. Phys. 4 (7) (2008) 532.
[32] A. Gupta, et al., Raman scattering from high-frequency phonons in supported n-graphene layer films, Nano Lett. 6 (12) (2006) 2667–2673.
[33] A.C. Ferrari, et al., Raman spectrum of graphene and graphene layers, Phys. Rev. Lett. 97 (18) (2006) 187401.
[34] T. Gruber, A. Grüneis, Ab initio calculations of carbon and boron nitride allotropes and their structural phase transitions using periodic coupled cluster theory, Phys. Rev. B 98 (13) (2018) 134108.
[35] W.J. Yu, et al., Ab initio study of phase transformations in boron nitride, Phys. Rev. B 67 (1) (2003), 014108.
[36] Z. Liu, et al., Open and closed edges of graphene layers, Phys. Rev. Lett. 102 (1) (2009), 015501.
[37] Y. Xu, X. Li, J. Dong, Infrared and Raman spectra of AA-stacking bilayer graphene, Nanotechnology 21 (6) (2010), 065711.
[38] P. Ordejón, E. Artacho, J.M. Soler, Self-consistent order-N density-functional calculations for very large systems, Phys. Rev. B 53 (16) (1996) R10441–R10444.
[39] D.M. Ceperley, B.J. Alder, Ground state of the electron gas by a stochastic method, Phys. Rev. Lett. 45 (7) (1980) 566–569.
[40] N. Troullier, J.L. Martins, Efficient pseudopotentials for plane-wave calculations, Phys. Rev. B 43 (3) (1991) 1993–2006.
[41] H.J. Monkhorst, J.D. Pack, Special points for Brillouin-zone integrations, Phys. Rev. B 13 (12) (1976) 5188–5192.
[42] R. Hundt, et al., Determination of symmetries and idealized cell parameters for simulated structures, J. Appl. Crystallogr. 32 (3) (1999) 413–416.
[43] A. Hannemann, et al., A new algorithm for space-group determination, J. Appl. Crystallogr. 31 (6) (1998) 922–928.
[44] F.D. Murnaghan, The compressibility of media under extreme pressures, Proc. Natl. Acad. Sci. 30 (9) (1944) 244.
[45] F. Birch, Finite elastic strain of cubic crystals, Phys. Rev. 71 (11) (1947) 809–824.
[46] C. Kürkçü, Z. Merdan, Ç. Yamçıçıer, Pressure-induced phase transitions, electronic, elastic and vibrational properties of zinc oxide under high pressure, Indian J. Phys. 93 (8) (2019) 979–989.
[47] C. Yamcicier, Z. Merdan, C. Kurkcu, Investigation of the structural and electronic properties of CdS under high pressure: an ab initio study, Can. J. Phys. 96 (2) (2018).
[48] H. Öztürk, M. Durandurdu, High-pressure phases of ZrO 2: an ab initio constant-pressure study, Phys. Rev. B 79 (13) (2009) 134111.
[49] C. Kürkçü, et al., Investigation of structural and electronic properties of β-HgS: molecular dynamics simulations, Chin. J. Phys. 56 (3) (2018) 783–792.
[50] J. Yin, et al., Direct or indirect semiconductor: the role of stacking fault in h-BN, Phys. B Condens. Matter 406 (11) (2011) 2293–2297.
[51] A. Candan, et al., Theoretical research on structural, electronic, mechanical, lattice dynamical and thermodynamic properties of layered ternary nitrides Ti2AN (A = Si, Ge and Sn), J. Alloy. Comp. 771 (2019) 664–673.
[52] X.-Y. Ren, et al., First-principles study of the crystal structures and physical properties of H18-BN and Rh6-BN, Phys. Lett. A 380 (46) (2016) 3891–3896.
[53] E. Kim, C. Chen, First-principles study of phase stability of BN under pressure, Phys. Lett. A 319 (3) (2003) 384–389.
[54] Y.-N. Xu, W.Y. Ching, Calculation of ground-state and optical properties of boron nitrides in the hexagonal, cubic, and wurtzite structures, Phys. Rev. B 44 (15) (1991) 7787–7798.
[55] L. Hromadová, R. Martoňák, Pressure-induced structural transitions in BN from ab initio metadynamics, Phys. Rev. B 84 (22) (2011) 224108.
[56] F.P. Bundy, R.H. Wentorf Jr., Direct transformation of hexagonal boron nitride to denser forms, J. Chem. Phys. 38 (5) (1963) 1144–1149.
[57] M. Ustundag, M. Aslan, B.G. Yalcin, The first-principles study on physical properties and phase stability of Boron-V (BN, BP, BAs, BSb and BBi) compounds, Comput. Mater. Sci. 81 (2014) 471–477.
[58] F.R. Corrigan, F.P. Bundy, Direct transitions among the allotropic forms of boron nitride at high pressures and temperatures, J. Chem. Phys. 63 (9) (1975) 3812–3820.
[59] V.I. Levitas, J. Hashemi, Y.Z. Ma, Strain-induced disorder and phase transformation in hexagonal boron nitride under quasi-homogeneous pressure: in situ X-ray study in a rotational diamond anvil cell, Europhys. Lett. 68 (4) (2004) 550–556.
[60] I. Hamdi, N. Meskini, Ab initio study of the structural, elastic, vibrational and thermodynamic properties of the hexagonal boron nitride: performance of LDA and GGA, Phys. B Condens. Matter 405 (13) (2010) 2785–2794.

[61] K. Karch, F. Bechstedt, Ab initio lattice dynamics of BN and AlN: covalent versus ionic forces, Phys. Rev. B 56 (12) (1997) 7404–7415.
[62] S.Q. Wang, H.Q. Ye, First-principles study on elastic properties and phase stability of III–V compounds, Phys. Status Solidi 240 (1) (2003) 45–54.
[63] R. Zhou, J. Dai, X. Cheng Zeng, Structural, electronic and mechanical properties of sp3-hybridized BN phases, Phys. Chem. Chem. Phys. 19 (15) (2017) 9923–9933.